CHEMISTRY OF MATERIALS

Article

pubs.acs.org/cm

Recyclable Hybrid Inorganic/Organic Magnetically Active Networks for the Sequestration of Crude Oil from Aqueous Environments

Jeniree A. Flores,[†] Adriana Pavía-Sanders,[†] Yingchao Chen,[‡] Darrin J. Pochan,[‡] and Karen L. Wooley*[,†]

[†]Department of Chemistry, Department of Chemical Engineering, Department of Materials Science and Engineering, Texas A&M University, College Station, Texas 77842, United States

[‡]Department of Materials Science and Engineering, University of Delaware, Newark, Delaware 19716, United States

Supporting Information

ABSTRACT: Hybrid inorganic/organic composite materials have been synthesized from the coupling of amine-functionalized iron oxide nanoparticles (amine-IONs) and pre-established shell cross-linked knedel-like (SCK) polymer nanoconstructs. The magnetically active hybrid networks (MHNs), composed of several interconnected SCKs bound to magnetically active amine-IONs, were designed for their application in the sequestration of hydrophobic contaminants from polluted environments. Initial assessment of the ability of the MHNs to capture complex pollutants, such as crude oil (oil), determined a loading capacity in the range of 3.5−4.5 mg of oil sequestered/mg of MHNs. The magnetic component of the hybrid nanoconstructs was exploited as a facile method of manipulation of the loaded networks, which allowed for the recovery of ca. 93% of the MHNs deployed in water, as well as ca. 90% recovery of the oil originally sequestered. Reutilization of these materials exhibited comparable efficiency after three cycles of remediation, which involved deployment, magnetic recovery, and organic washes to remove the cargo. The multiple characteristics of these materials could be exploited in the cleaning of water contaminated during the process of drilling, extraction, and transport of crude oil, among other applications.

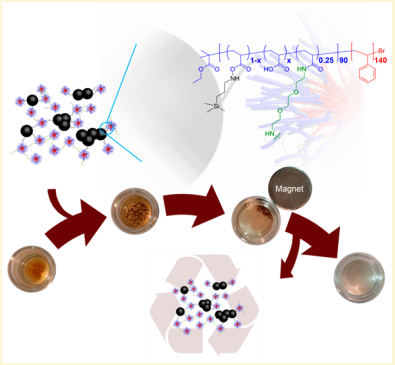

INTRODUCTION

The deposition of chemicals and particles, as well as industrial, agricultural, and residential waste into major bodies of water poses a danger to the growth and development of healthy biological populations. Among the pollutants that severely affect aquatic environments are hydrocarbons deposited in the water during the drilling, extraction, and transport of crude oil. One of the main sources of contamination is oil spills, of which ca. 20 000 were reported to the U.S. Coast Guard National Response Center in 2014,[1] of varying severities and requiring varying extents of cleanup efforts; higher numbers are expected as global spills are taken into consideration. In cases of large-volume spills, a remediation routine involving the use of mechanical methods, such as booms, skimmers, or suction, is utilized to remove the bulk of the oil discharged.[2] However, the use of these mechanical methods becomes inefficient for the removal of low concentrations of oil, better known as sheen, which appears as a thin layer of oil ca. 0.04−50 μm thick on the surface of the water.[3]

An additional source of contamination is produced water (PW), which is a mixture of water trapped in underground formations and the water injected into the reservoir to facilitate drilling and extraction of oil during hydraulic fracturing (fracking) practices. Although this water has a variety of contaminants, the content of hydrocarbons is of primary concern, notably the suspended oil present, which can be reminiscent of sheen. Between 2010 and 2011, the water produced by the Marcellus formation, which encompasses parts of the states of New York, Pennsylvania, Ohio, and West Virginia, was estimated to be 1.3 billion gallons in Pennsylvania alone.[4,5] If PW could be cleaned to achieve environmental standards, it could be reutilized in areas such as underground injection, irrigation, and other industrial uses (e.g., power plant makeup water and vehicle washing), diminishing its environmental impact.[6]

Recently, many advances have focused on designing materials for the separation of oil/water mixtures, such as sponges,[7−10] nanowires,[11] hydrogels,[12−14] fibers,[15] organic−inorganic composite membranes,[16,17] and nanoparticles.[18−20] However, despite their remarkable performance, many rely on manual labor for the manipulation and removal of the oil-loaded materials, making them less desirable for the remediation of contaminated water, because of financial and feasibility constraints. To address this issue, nanomaterials with an added magnetic component have been synthesized to allow for their facile recovery once loaded by the oil contaminant. For instance, Zhu and co-workers synthesized polyurethane foams modified with polytetrafluoroethylene (PTFE) and iron oxide nanoparticles (IONs), which were successful in the removal of mineral oil from an aqueous solution via the magnetic handling

Received: April 24, 2015
Revised: April 28, 2015
Published: May 7, 2015

DOI: 10.1021/acs.chemmater.5b01523
Chem. Mater. 2015, 27, 3775−3782

Scheme 1. Schematic Representation of (a) the Synthesis of SCKs and (b) the Covalent Binding of SCKs to Amine-Functionalized IONs via Amidation

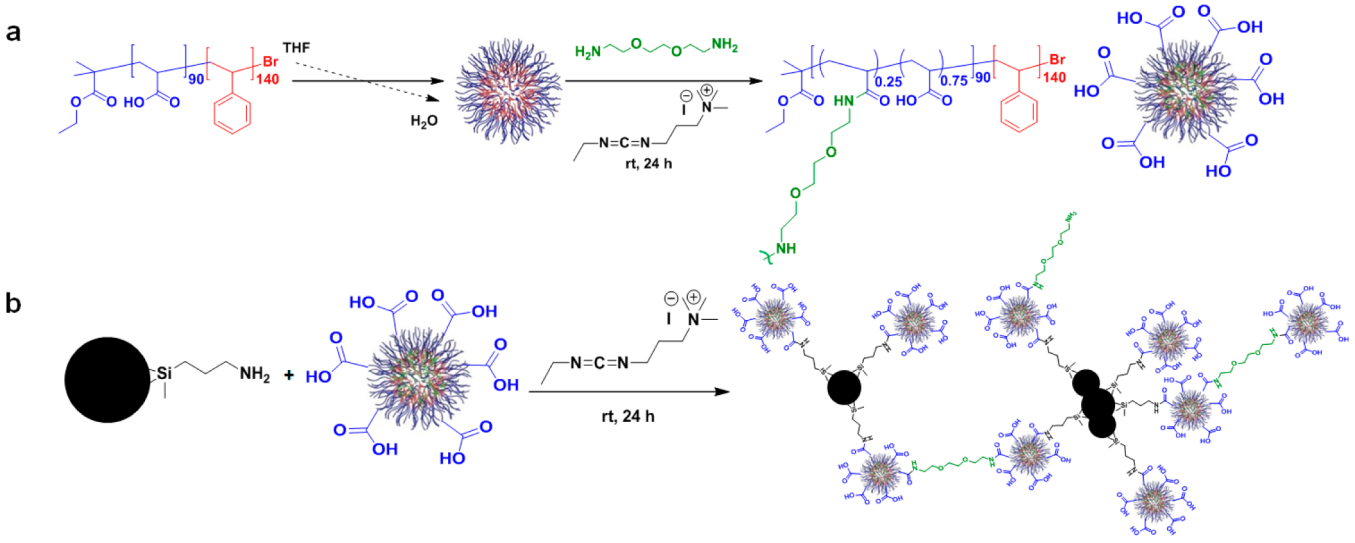

of the foam.[8] Similarly, the Pan group developed highly hydrophobic IONs coated with polysiloxane, which showed a high absorbing efficiency that was >10 times greater than the weight of the material.[19] Despite the remarkable performance of these materials, their hydrophobic nature represented a limitation for the removal of submerged oil. To address this issue, Lead and co-workers synthesized water-dispersible polyvinylpyrrolidone (PVP)-coated IONs capable of removing crude oil from a water/oil mixture at a ratio of 1:2.6 (oil:PVP-IONs).[20] Recently, our group has synthesized magnetic shell cross-linked knedel-like (MSCK) nanoparticles, which combined amphiphilic polymers (to allow for aqueous dispersibility and crude oil sequestration) with magnetic nanoparticles (to provide for magnetic recovery) in a robust nanoscopic structure. These organic/inorganic cross-linked micellar structures, composed of poly(acrylic acid)-*block*-polystyrene (PAA-*b*-PS) block copolymers and 8 nm IONs, had a core−shell morphology, overall dimensions of ca. 70 nm and contained large numbers of IONs within the amphiphilic block copolymer framework. The MSCKs were capable of sequestering crude oil from aqueous dispersions at a 1:10 (nanoparticle:oil) ratio by weight and exhibited quantitative recyclability.[21] With the significant advancement in the synthesis of remediating nanomaterials capable of sequestering buoyant and submerged oil made possible by the MSCK amphiphilic character, we anticipated that producing similar polymer−nanoparticle assemblies by a stagewise protocol would allow for definition of the composition and morphology to improve understanding of the structure-property-function relationships and optimize performance.

Consequently, we sought the development of compartmentalized materials assembled from prefabricated shell cross-linked knedel-like (SCK) nanoparticles covalently bound to magnetic inorganic substrates. As opposed to the MSCK structure, these hybrid materials were designed initially to present multiple copies of SCK polymer nanoparticles around a central magnetic inorganic nanoparticle core. It was expected that this morphology would allow for the sequestration of a diverse number of complex contaminants through tailoring of the polymeric SCK components. As an initial proof of concept, we report the synthesis of magnetically active hybrid networks (MHNs) from the conjugation of PAA-*b*-PS SCK nanoparticles to similarly sized amine-functionalized IONs (amine-IONs). Rather than the idealized central inorganic and satellite organic nanoparticle structure, complex multiparticle MHNs were obtained. Their application toward the remediation of water contaminated with complex pollutants such as crude oil is demonstrated, as well as their potential for recovery of the pollutants and recyclability of the materials.

EXPERIMENTAL SECTION

Synthesis of Magnetically Active Hybrid Networks (MHNs). A 250 mL vial was charged with a stir bar and a solution of SCKs (12 equiv, 70 mL, 0.27 mg/mL, 20 mg, 62 μmol of available acrylic acid units). A solution of amine-functionalized iron oxide nanoparticles (amine-IONs, 1 equiv, 22.6 mL, 0.15 mg/mL, 3.4 mg, 5.2 μmol of ligand) was added dropwise to the reaction mixture and it was allowed to stir for ca. 5 min, after which a solution of 1-[3′-(dimethylamino)-propyl]-3-ethylcarbodiimide methiodide (EDCI) (13.5 mg, 45.4 μmol, 8.8 equiv, as a 7.5 mL aqueous solution at a concentration of 1.8 mg/mL) was added via a syringe pump at a rate of 0.25 mL/min. The reaction was allowed to stir for 24 h, followed by centrifugation at 10 000 rpm for 5 min. The brown precipitate was resuspended in 15 mL of nanopure water with the aid of sonication and vortexing, this process was repeated twice. The supernatant was collected and centrifuged 2 more times with the aim of removing as much precipitate as possible. After centrifugation, the supernatant was collected, placed in presoaked membrane dialysis tubing (MWCO 12−14 kDa), and dialyzed against nanopure water for 3 days. Following dialysis, the suspension of MHNs and the supernatant were combined (due to similar structures being observed by TEM) and lyophilized to afford 16 mg of a light brown powder in 69% yield. IR: ν = 3685−2545, 3110−3010, 3010−2835, 2385−2300, 1960−1850, 1720, 1640, 1600, 1550, 1490, 1450, 1390, 1365, 1350, 1260, 1210, 1180, 1140, 1095, 1070, 1030, 965, 905, 800, 755, 700 cm^{-1}. TGA: T_{onset} = 30 °C. $T_{decomposition}$: 30−100 °C, 4% mass loss; 100−210 °C, 5% mass loss; 210−250 °C, 9% mass loss; 290−375 °C, 48% mass loss; and 410−470 °C, 16% mass loss (with 18% of the mass remaining).

DOI: 10.1021/acs.chemmater.5b01523
Chem. Mater. 2015, 27, 3775−3782

Oil Capture Experiments. Weathered crude oil from the Texas−Oklahoma pipeline (light sweet crude oil) was added to a vial containing nanopure water (3 mL) and the weight of the oil was recorded. Subsequently, powdered MHNs were added to the vial and they were allowed to rest with minimal movement. After ca. 1 h, the loaded material was separated via exposure to an external magnetic field for ca. 2 min, followed by decanting of the contaminated media for oil extraction. The original vial was washed twice with nanopure water (2 mL) in order to remove most of the water/oil mixture remaining. The vial was dried and its mass recorded in order to determine the mass of oil remaining in the original container. Subsequently, the oil present in the polluted environment was extracted using diethyl ether; the organic fractions were collected in order to evaporate the solvent and to record the mass of the extracted oil. In addition, the water fraction was collected and lyophilized in order to determine the presence of any residual mass in the aqueous phase.

Oil Recovery Experiments. The loaded MHNs were transferred into a preweighed clean vial, followed by the addition of diethyl ether (2 mL). The sample was vortexed for ca. 30 s to wash the oil captured. The nanoparticles were separated from the mixture by exposure to an external magnetic field for ca. 1 min, followed by decanting of the solvent. This process was repeated twice, with a colorless solution indicating extraction of the majority of the oil from the nanoparticles. The decanted mixture was allowed to dry and the mass of oil extracted from the nanoclusters was measured.

■ RESULTS AND DISCUSSION

Synthesis and Characterization of Magnetically Active Hybrid Networks (MHNs). The MHNs were synthesized in a two-step manner (Scheme 1). First, the preparation of the SCKs was performed from a modified literature procedure ($D_{h(n)}$ = 18 ± 5 nm, as measured by dynamic light scattering (DLS); see Figure S1 in the Supporting Information),[22,23] followed by the covalent binding of these pre-established polymeric nanoparticles to amine-IONs ($D_{h(n)}$ = 50 ± 15 nm; see Figure S2 in the Supporting Information) via an amidation reaction between the acrylic acid functionalities of the hydrophilic shell of the SCKs and the amine moieties on the surface of the IONs in the presence of EDCI. After purification by magnetic separation and dialysis of the supernatant, the composite material was characterized through transmission electron microscopy (TEM), infrared (IR) spectroscopy, and thermogravimetric analysis (TGA). TEM imaging revealed a hybrid network composed of agglomerated IONs coupled to multiple SCKs (Figure 1).

The use of phosphotungstic acid (PTA) as a staining agent during TEM analysis improved the contrast to allow for the observation of the SCKs (light globular structures in Figure 1a) which would otherwise be difficult to visualize. However, staining also introduced artifacts[24] and provided ambiguity when determining whether the areas of high contrast (black areas in Figure 1a) corresponded to the transmission generated by amine-IONs or to areas of high concentrations of stain. In addition, the process of drying the sample on a TEM grid led to ambiguities of whether the SCK clusters were due to a drying pattern or were, in fact, representative of interconnections between SCK particles. Although the nanoparticles were composed of C, H, O, and N atoms, all of which have relatively low and similar atomic numbers (Z) and thus provide poor mass−thickness contrast by TEM,[25] cryogenic TEM

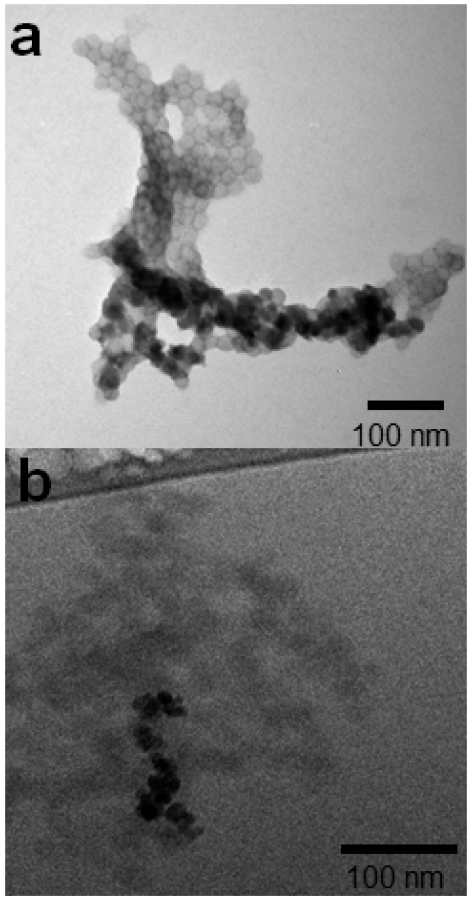

Figure 1. (a) TEM image of MHNs after staining with phosphotungstic acid (PTA) and (b) cryo TEM image of MHNs.

(cryo-TEM) was able to confirm the presence of agglomerates of amine-IONs bound to several interconnected SCKs (Figure 1b). We hypothesized that the SCK-SCK interactions have a covalent character, facilitated by interparticle amidation reactions between EDCI-activated carboxylic acids with residual amino groups in the shells of the nanoparticles, following the initial intraparticle shell cross-linking step. This hypothesis was corroborated by our control experiments, which were performed by adding EDCI to a solution of SCKs. TEM micrographs (Figure S3 in the Supporting Information) revealed the formation of SCK clusters identical to those formed during the synthesis of the MHNs, which were not present before the second addition of EDCI and could have only formed if the residual amino groups in the shells of the SCKs reacted with residual carboxylic acid units, since no other source of amines was present in the system. Moreover, to confirm the covalent nature of the MHNs throughout the inorganic and organic components, a series of control experiments was conducted (see Figure 2, as well as Figure S4 in the Supporting Information) to compare the MHN structures collected from the precipitate and supernatant (see Figures 2a and 2b, as well as Figure S4 in the Supporting Information), following the addition of the EDCI coupling agent with analogous physical mixtures collected in the absence of the carbodiimide (see Figures 2c and 2d, as well as Figure S4 in the Supporting Information). We cannot explain why SCK-SCK coupling proceded during the amidation conditions employed for conjugation with the amine-IONs, but not during the intramicellar cross-linking reaction to establish the

DOI: 10.1021/acs.chemmater.5b01523
Chem. Mater. 2015, 27, 3775−3782

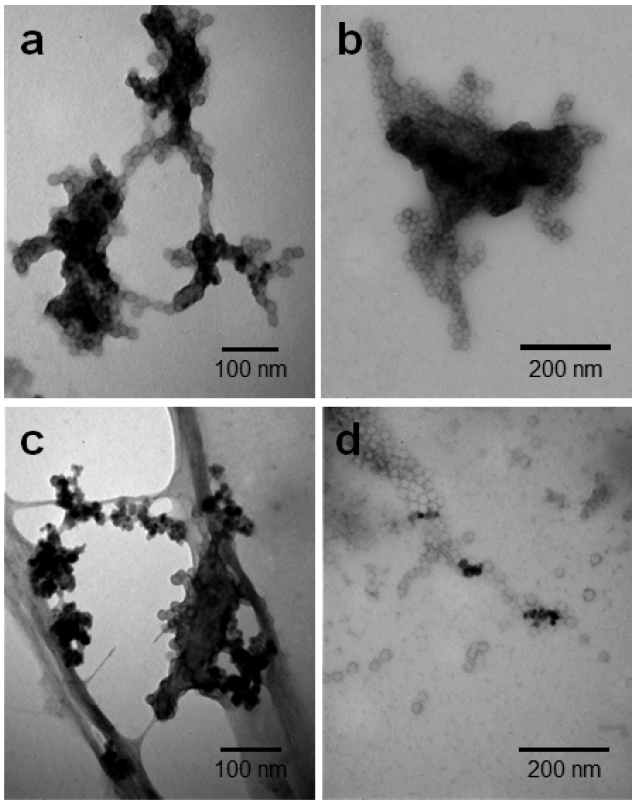

Figure 2. TEM images of the (a) precipitate and (b) supernatant of the MHNs, compared to the (c) precipitate and (d) supernatant of a physical mixture of SCKs and amine-IONs.

SCKs. Originally, the workup and purification process involved separate treatments for the supernatant and precipitate obtained from centrifugation. With detailed TEM analyses, it was found that both the precipitate and supernatant contained the same type of MHN structures; therefore, the samples were combined for further analyses and crude oil capture studies.

Infrared (IR) spectroscopy was used in addition to TEM analysis to monitor structural changes in the composition of the SCKs (Figure 3a). The band at ca. 1710 cm^{-1} corresponds to the carbonyl stretch for the acrylic acid pendant groups of the SCKs, while the signals at ca. 1640 cm^{-1} and ca. 1560 cm^{-1} are characteristic of the amide functional group and are an indication of the cross-linking of the shell, which was performed to afford stability to the nanoparticles.[26] However, this second amidation reaction for the coupling of the inorganic and organic components revealed no significant changes to the IR absorbance bands between the SCKs and MHNs. This lack of measurable structural changes could be attributed to the use of amidation chemistries for both the cross-linking and coupling of the SCKs and amine-IONs.

TGA was also performed in order to gain a better understanding of the thermal stability and composition of the hybrid nanoconstructs. Comparison of the thermographs of amine-IONs, MHNs, and SCKs (Figure 3b) revealed a lower decomposition temperature for the MHNs (ca. 190 °C) when compared to that of the SCKs (ca. 230 °C). This reduction of the stability of the hybrid networks could be due to the interconnection between the inorganic particles and the SCKs, which form an intricate network that can be affected by the thermal conductivity of the amine-IONs, or by metal-catalyzed oxidative degradation, typically observed in metal/polymer nanocomposites.[27−30] Moreover, the percentage of amine-IONs present in the MHNs was also assessed by TGA, which revealed an inorganic loading of ca. 16% by mass to the hybrid material, which is consistent with the 15 ± 1 wt % amine-IONs:SCK feed ratio used in the synthesis of the MHNs.

Qualitative and Quantitative Sequestration of Crude Oil by the MHNs. Following the complete characterization of the novel hybrid networks, the ability of the MHNs to sequester complex hydrophobic pollutants was assessed qualitatively. First, crude oil from the Texas−Oklahoma Enbridge pipeline was weathered according to a pre-established procedure,[31] and then added to nanopure water in order to mimic sheen contamination. Second, the lyophilized MHNs were deployed onto the polluted environment in a powder form at initial oil:MHN ratios of 2:1, 4:1, 6:1, and 8:1. Immediately after deployment, a color change from light tan to darker brown/black was observed for the MHNs, indicating that the particles had come into contact with the oil and had possibly taken up the pollutant (see Figure S5 in the Supporting Information). After ca. 1 h, the loaded nanoparticles were subjected to an external magnet (neodymium magnet, 90 lb pull). Because of the high magnetic response of the large conglomerates of oil and nanoparticles, these species were quickly, within a matter of seconds, attracted to the magnet. However, the smaller droplets of oil required a longer time to

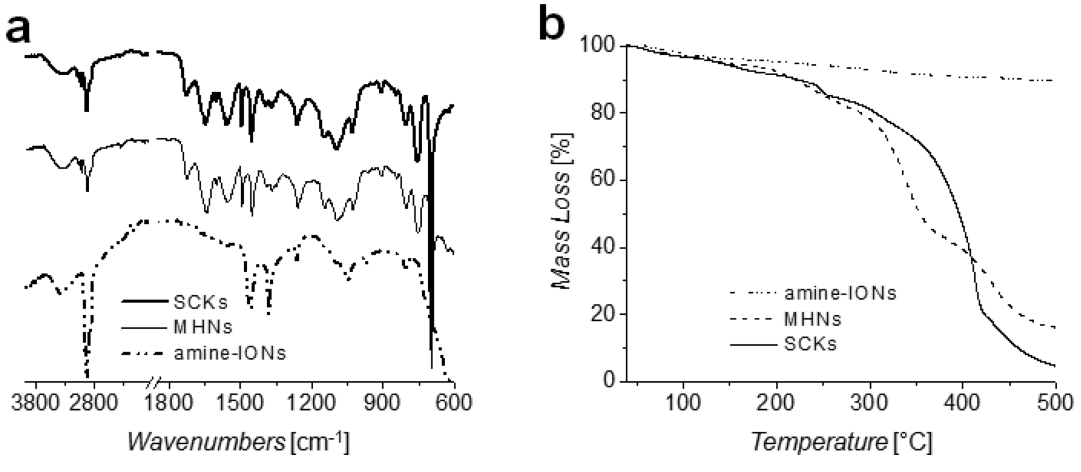

Figure 3. (a) Infrared (IR) spectra of SCKs, MHNs, and amine-IONs; (b) TGA thermographs of amine-IONs, MHNs, and SCKs.

DOI: 10.1021/acs.chemmater.5b01523
Chem. Mater. 2015, 27, 3775−3782

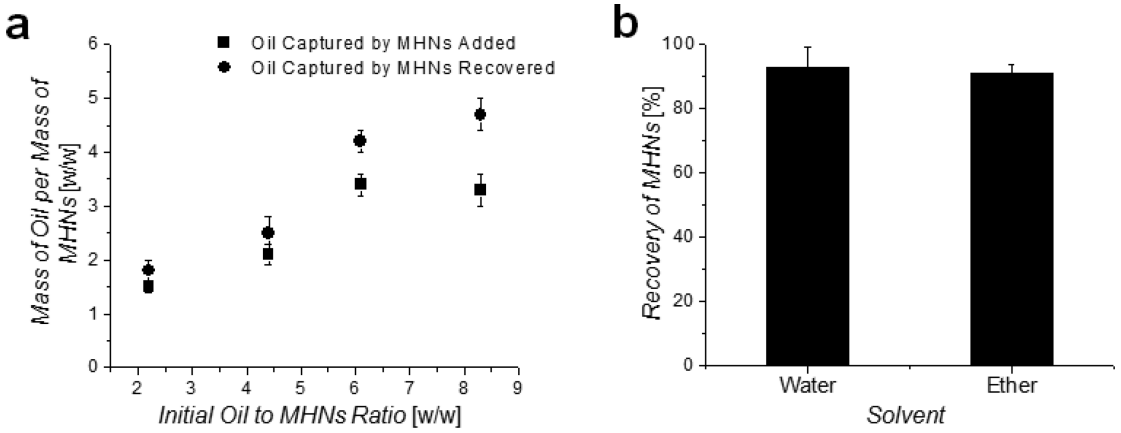

Figure 4. (a) Loading capacity ratio of the MHNs, calculated as the mass of oil (mg) captured per mg of MHNs added (squares) and the mass of oil (mg) captured per mg of MHNs recovered (circles); (b) magnetic recovery of MHNs after deployment in water and diethyl ether.

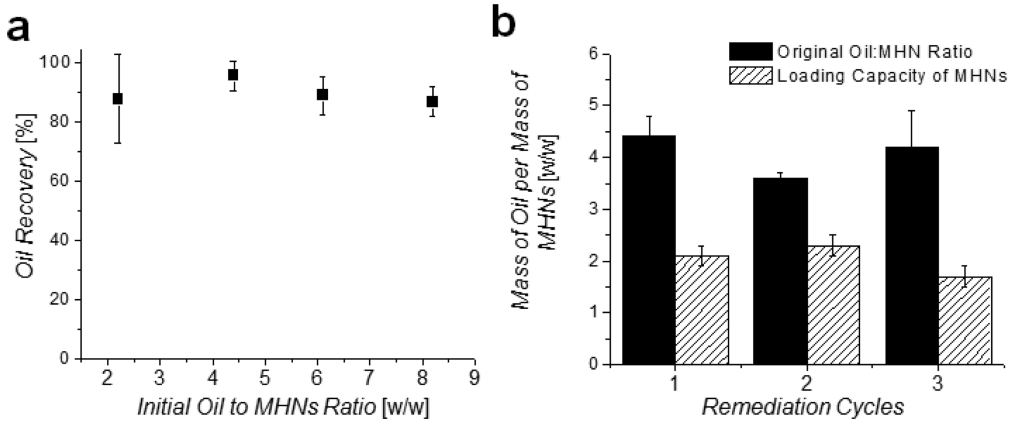

Figure 5. (a) Percent oil recovery as a result of the washing of pollutant-loaded nanoparticles, and (b) recyclability of the MHNs assessed as a comparison between the loading capacity of the MHNs after multiple remediation cycles, and the original oil:MHNs ratio.

be completely removed from the resting contaminated water; therefore, magnetic separation was performed for a total of 2 min. The contaminants remaining in the polluted mixture were decanted and compared to control samples containing comparable amounts to the initial oil. Qualitatively, it could be observed that the MHNs were capable of sequestering most of the pollutants initially present in the water (Figure S5 in the Supporting Information).

The qualitative assesment of the sequestration of hydrophobic contaminats by the MHNs was followed by a quantitative determination of their loading capacity, which was achieved through a masss balance method. The mass of oil captured by the MHNs was calculated gravimetrically by measuring the initial mass of oil added into the pristine water, the mass of oil remaining in the vial after transfer of the polluted solution and oil-containing MHNs, the mass of oil not captured from the polluted solution (analyzed after diethyl ether extraction from the water), and the mass of oil extracted with diethyl ether after MHNs deployment and recovery. The loading capacity of the materials was calculated as the ratio of the mass of oil sequestered (in units of mg/mg of MHNs). For the initial ratio of 2.2:1 (oil:MHN), it was determined that 1.5 mg of oil were captured per 1 mg of MHNs. For the subsequent ratios of 4.4:1, 6.1:1, and 8.3:1, the loading capacities were found to be 2.1:1, 3.4:1, and 3.3:1, respectively (Figure 4a).

Furthermore, in order to address the concern that there may be populations of the interparticle cross-linked networks comprised only of SCKs, without having the composite structure together with amine-IONs, the magnetic recovery of MHNs was assessed. The experiments indicated that ca. 93% of the MHNs originallly deployed in water could be recovered with the use of an external magnet (Figure 4b). Therefore, the loading capacity of the hybrid networks was also calculated as the ratio of the mass of oil sequestered (in units of mg/mg of MHNs recovered). Through this approach, at the lower ratios of 2.2:1 and 4.4:1, quantitative recovery of the MHNs occurred, as observed by the fact that no significant difference was observed between the captured oil values calculated using the two methods (Figure 4a). However, for higher loading ratios, significant differences were observed. The effective amount of captured oil was higher, when taking into account the loss of fractions of the MHN samples during the procedures involving high proportions of oil (6.1:1 and 8.3:1), with a maximum oil sorption determined to be 4.7 mg of oil/mg of MHNs recovered. These differences can be attributed to an increase in the difficulty with which the pollutant-loaded networks were magnetically manipulated and recovered as the proportion of oil increased. As the concentration of oil in the polluted water was increased, it became more cumbersome to remove the oil-loaded networks and thus, to accurately calculate the loading capacity. In fact, attempts to further challenge the system with an initial loading ratio of 10:1 were unsuccessful, because it was

DOI: 10.1021/acs.chemmater.5b01523
Chem. Mater. 2015, 27, 3775−3782

not possible to remove the loaded MHNs from the resting polluted environment without leaching oil back into the system. Thus, by taking these observations into consideration, it can be determined that the maximum loading capacity falls in a range of ca. 3.5−4.5 mg of oil/mg of MHNs.

Oil Cargo Removal and Recyclability of MHNs. The recyclability of the MHNs was first addressed by removing the loaded pollutants through a wash with an organic solvent. Diethyl ether was selected as the organic solvent, since preliminary data indicated that it could remove the oil without solubilizing the MHNs. Moreover, control experiments were conducted to determine the magnetic recovery of the networks after the organic wash, which revealed that ca. 90% of the MHNs could be successfully retrieved (Figure 4b). The washing of the loaded nanoparticles was performed by redispersion in diethyl ether, followed by 30 s of vortexing. A change in the color of the solvent from colorless to light yellow/brown inidicated the removal of oil from the MHNs. Further confirmation of the removal of oil was provided by the change in the color of the nanoparticles from black (pollutant-loaded) to brown (similar color to the pristine system). The MHNs were removed magnetically from the diethyl ether/oil mixture, followed by evaporation of the solvent, which allowed for the calculation of the amount of oil recovered from the networks; this amount was determined to be ca. 90% of the amount of oil initially sequestered (Figure 5a).

The extraction of the loaded pollutants was followed by the reutilization of MHNs for the sequestration of oil. The washed nanoparticles were redeployed into contaminated media and were exposed to the same procedure as previously stated for the sequestration and quantification of oil removal. The loading capacity of the reused MHNs was assesed for three cycles at an initial oil:MHNs ratio of 4:1 (Figure 5b). The ratio calculated across all cycles was determined to be ca. 2:1, which suggests little to no reduction of the efficiency of the MHNs following three cycles of deployment and organic washing. These data indicate that the MHNs system could be effective and viable for the sequestration and recovery of crude oil from water.

Interfacial Tension Measurements. In addition to synthesizing novel complex materials capable of removing hydrophobic pollutants from aqueous environments, we were also interested in understanding the mechanism of interaction between the pollutants and the MHNs. Our first step in this direction has been the determination of the interfacial tension (γ) between the oil and a suspension of MHNs via a pendant drop method. The interfacial tension of a drop of oil (density = 0.8234 mg/mL) in a 0.25 mg/mL aqueous suspension of MHNs was measured to be 19.4 ± 0.6 mN/m (see Table 1), which represents a 23.3% reduction in the interfacial tension of the oil, when compared to its value in water (25.3 ± 0.2 mN/m). These results indicate an increased affinity of the oil for the suspension of MHNs, and are indicative of the possible formation of an emulsion between the oil and the water phases, estabilized by the MHN particles, as seen in the process of Pickering emulsification.[32] Although more data are required in order to support this hypothesis, the formation of Pickering emulsions could indicate that the mechanism of loading is not limited to oil sorption into the hydrophobic core of the SCKs composing the magnetically active networks, but includes the formation of magnetically active droplets in water.[33−36] Moreover, we also measured γ for model aromatic and aliphatic contaminants in a suspension of MHNs, in order to determine if there is an increased affinity for one of the components of oil. The surface tension of toluene (model aromatic contaminant) was reduced from 35.2 ± 0.4 mN/m (water) to 19.1 ± 0.2 mN/m (MHNs), while the interfacial tension of decane (model aliphatic pollutant) was decreased from 52.3 ± 0.5 mN/m (water) to 37.7 ± 0.8 mN/m (MHNs). Analysis of these data showed that γ for toluene was reduced by 45.5% while that of decane was reduced by 27.9%, which could indicate an increased affinity for the aromatic components of the oil, or for smaller molecules over long-chain aliphatic hydrocarbons. Even though these data are not conclusive, ongoing experiments are focused on determining any preferential sequestration of oil components by MHNs.

Table 1. Interfacial Tension Values for Hydrophobic Organic Pollutants in Water and MHNs

	Media		
drop solvent	water (mN/m)	MHNs (mN/m)	% difference
toluene	35.2 ± 0.4	19.1 ± 0.2	45.7
decane	52.3 ± 0.5	37.7 ± 0.8	27.9
crude oil	25.3 ± 0.2	19.4 ± 0.6	23.3

CONCLUSIONS

The construction of magnetically active hybrid networks for the removal of complex hydrophobic pollutants from water provided an exciting addition to the morphologies currently available for remediation. The maximum loading capacity calculated lies in the range of ca. 3.5−4.5 mg of oil/mg of MHNs used, which is comparable to the capacity of existing nanotechnology. The high percent of recovery of the sequestered oil, as well as the reutilization of the MHNs with quantitative efficiency, are two factors that could lower the cost associated with production and use of the MHNs in environmental remediation. These characteristics, coupled with the MHNs' capabilities for water compatibility, magnetic manipulation and easy recovery of the cargo, also expand their possible applications to new challenges encountered by the constant search for energy sources, such as enhanced oil recovery. Although this novel system demonstrated a lower oil uptake when compared to the MSCK system,[21] we have found unique insights into the mechanism of interaction between the MHNs and hydrophobic pollutants that significantly improve our understanding of these materials. Moreover, their uncomplicated assembly method provides unlimited opportunities to expand the scope of these materials, notably through the tailoring of the SCK component for specific pollutants and applications. Ongoing studies are focused on altering the polymeric domains prior to assembly onto the inorganic component, to afford finely tuned SCKs that could sequester particular pollutants encountered in diverse scenarios. In addition, multiple SCKs of different compositions could be coupled onto the inorganic magnetically active vehicles, thus providing highly diverse materials with minimal synthetic modifications.

ASSOCIATED CONTENT

Supporting Information

Characterization techniques; detailed procedures and characterization data for the synthesis of the amphiphilic block copolymers, micelles, SCKs and MHNs, and digital photographs of the MHNs absorbing crude oil from water. The

DOI: 10.1021/acs.chemmater.5b01523
Chem. Mater. 2015, 27, 3775−3782

Supporting Information is available free of charge on the ACS Publications website at DOI: 10.1021/acs.chemmater.5b01523.

AUTHOR INFORMATION

Corresponding Author

*E-mail: wooley@chem.tamu.edu.

Notes

The authors declare no competing financial interest.

ACKNOWLEDGMENTS

We gratefully acknowledge financial support from the National Science Foundation (under Grant Nos. DMR-1105304, DMR-1309724, and DMR-1309813), and the Welch Foundation, through the W.T Doherty–Welch Chair in Chemistry (under Grant No. A-0001). Enbridge Energy Partners, LP is gratefully acknowledged for their donation of the West Texas crude oil, the Schechter group in the Petroleum Engineering Department at Texas A&M University for providing the instrumentation necessary to perform the interfacial tension experiments, and the Microscopy Imaging Center (MIC) at Texas A&M University for providing accessibility to TEM instrumentation.

REFERENCES

(1) *Reports from the United States Coast Guard National Response Center*; available via the Internet at http://www.nrc.uscg.mil/Default.aspx (accessed Feb. 2015).

(2) U.S. Environmental Protection Agency. *Oil Spill Response Techniques*; available via the Internet at http://www.epa.gov/emergencies/content/learning/oiltech.htm (accessed Sept. 2013).

(3) *Identification of Oil on Water: Aerial observation and identification guide*; available via the Internet at http://www.scribd.com/doc/220918003/AMSA-IDENTIFICATION-of-OIL-on-WATER-Aerial-Observation-and-Identification-Guide (accessed Nov. 2014).

(4) Rahm, B. G.; Bates, J. T.; Bertoia, L. R.; Galford, A. E.; Yoxtheimer, D. A.; Riha, S. J. Wastewater Management and Marcellus Shale Gas Development: Trends, drivers, and planning implications. *J. Environ. Manage.* **2013**, *120*, 105–113.

(5) Lutz, B. D.; Lewis, A. N.; Doyle, M. W. Generation, Transport, and Disposal of Wastewater Associated with Marcellus Shale Gas Development. *Water Resour. Res.* **2013**, *49*, 647–656.

(6) Rahm, B. G.; Riha, S. J. Evolving Shale Gas Management: Water resource risks, impacts, and lessons learned. *Environ. Sci.: Processes Impacts* **2014**, *16*, 1400–1412.

(7) Zhu, Q.; Pan, Q.; Liu, F. Facile Removal and Collection of Oils from Water Surfaces through Superhydrophobic and Superoleophilic Sponges. *J. Phys. Chem. C* **2011**, *115*, 17464–17470.

(8) Calcagnile, P.; Fragouli, D.; Bayer, I. S.; Anyfantis, G. C.; Martiradonna, L.; Cozzoli, P. D.; Cingolani, R.; Athanassiou, A. Magnetically Driven Floating Foams for the Removal of Oil Contaminants from Water. *ACS Nano* **2012**, *6*, 5413–5419.

(9) Gui, X.; Cao, A.; Wei, J.; Li, H.; Jia, Y.; Li, Z.; Fan, L.; Wang, K.; Zhu, H.; Wu, D. Soft, Highly Conductive Nanotube Sponges and Composites with Controlled Compressibility. *ACS Nano* **2010**, *4*, 2320–2326.

(10) Chen, N.; Pan, Q. Versatile Fabrication of Ultralight Magnetic Foams and Application for Oil–Water Separation. *ACS Nano* **2013**, *7*, 6875–6883.

(11) Yuan, J.; Liu, X.; Akbulut, O.; Hu, J.; Suib, S. L.; Kong, J.; Stellacci, F. Superwetting Nanowire Membranes for Selective Absorption. *Nat. Nanotechnol.* **2008**, *3*, 332–336.

(12) Cong, H.; Ren, X.; Wang, P.; Yu, S. Macroscopic Multifunctional Graphene-Based Hydrogels and Aerogels by a Metal Ion Induced Self-Assembly Process. *ACS Nano* **2012**, *6*, 2693–2703.

(13) Korhonen, J. T.; Kettunen, M.; Ras, R. H.; Ikkala, O. Hydrophobic Nanocellulose Aerogels as Floating, Sustainable, Reusable, and Recyclable Oil Absorbents. *ACS Appl. Mater. Interfaces* **2011**, *3*, 1813–1816.

(14) Basak, S.; Nanda, J.; Banerjee, A. A New Aromatic Amino Acid Based Organogel for Oil Spill Recovery. *J. Mater. Chem.* **2012**, *22*, 11658–11664.

(15) Yang, Y.; Zhang, X.; Wang, Z. Oilfield Produced Water Treatment with Surface-Modified Fiber Ball Media Filtration. *Water Sci. Technol.* **2002**, *46*, 165–170.

(16) Li, Y. S.; Yan, L.; Xiang, C. B.; Hong, L. J. Treatment of Oily Wastewater by Organic–Inorganic Composite Tubular Ultrafiltration (UF) Membranes. *Desalination* **2006**, *196*, 76–83.

(17) Maguire-Boyle, S. J.; Barron, A. R. A New Functionalization Strategy for Oil/Water Separation Membranes. *J. Membr. Sci.* **2011**, *382*, 107–115.

(18) Zhu, L.; Li, C.; Wang, J.; Zhang, H.; Jian, Z.; Shen, Y.; Li, C.; Wang, C.; Xie, A. A Simple Method to Synthesize Modified Fe_3O_4 for the Removal of Organic Pollutants on Water Surface. *Appl. Surf. Sci.* **2012**, *258*, 6326–6330.

(19) Zhu, Q.; Tao, F.; Pan, Q. Fast and Selective Removal of Oils from Water Surface via Highly Hydrophobic Core-Shell Fe_2O_3@C Nanoparticles Under Magnetic Field. *ACS Appl. Mater. Interfaces* **2010**, *2*, 3141–3146.

(20) Palchoudhury, S.; Lead, J. R. A Facile and Cost-Effective Method for Separation of Oil–Water Mixtures Using Polymer-Coated Iron Oxide Nanoparticles. *Environ. Sci. Technol.* **2014**, *48*, 14558–14563.

(21) Pavía-Sanders, A.; Zhang, S.; Flores, J. A.; Sanders, J. E.; Raymond, J. E.; Wooley, K. L. Robust Magnetic/Polymer Hybrid Nanoparticles Designed for Crude Oil Entrapment and Recovery in Aqueous Environments. *ACS Nano* **2013**, *7*, 7552–7561.

(22) Zhang, S.; Li, Z.; Samarajeewa, S.; Sun, G.; Yang, C.; Wooley, K. L. Orthogonally Dual-Clickable Janus Nanoparticles *via* a Cyclic Templating Strategy. *J. Am. Chem. Soc.* **2011**, *133*, 11046–11049.

(23) O'Reilly, R. K.; Joralemon, M. J.; Wooley, K. L.; Hawker, C. J. Functionalization of Micelles and Shell Cross-linked Nanoparticles Using Click Chemistry. *Chem. Mater.* **2005**, *17*, 5976–5988.

(24) Handlin, D. L.; Thomas, E. L. Phase Contrast Imaging of Styrene–Isoprene and Styrene–Butadiene Block Copolymers. *Macromolecules* **1983**, *16*, 1514–1525.

(25) Williams, D. B.; Carter, C. B. *Transmission Electron Microscopy: A Textbook for Materials Science*, 2nd Edition; Springer Science +Business Media, LLC: New York, 2009; Vol. 3, pp 373–374.

(26) Huang, H.; Kowalewski, T.; Remsen, E. E.; Gertzmann, R.; Wooley, K. L. Hydrogel-Coated Glassy Nanospheres: A novel method for the synthesis of shell cross-linked knedels. *J. Am. Chem. Soc.* **1997**, *119*, 11653–11659.

(27) Rancourt, J. D.; Taylor, L. T. Preparation and Properties of Surface-conductive Polyimide Films via in situ Codeposition of Metal Salts. *Macromolecules* **1987**, *20*, 790–795.

(28) Chiang, P.-C.; Whang, W.-T. The Synthesis and Morphology Characteristic Study of BAO-ODPA Polyimide/TiO_2 Nano Hybrid Films. *Polymer* **2003**, *44*, 2249–2254.

(29) Hsu, S.-C.; Whang, W.-T.; Hung, C.-H.; Chiang, P.-C.; Hsiao, Y.-N. Effect of the Polyimide Structure and ZnO Concentration on the Morphology and Characteristics of Polyimide/ZnO Nanohybrid Films. *Macromol. Chem. Phys.* **2005**, *206*, 291–298.

(30) Agarwal, T.; Gupta, K. A.; Alam, S.; Zaidi, M. G. H. Fabrication and Characterization of Iron Oxide Filled Polyvinyl Pyrrolidone Nanocomposites. *Int. J. Compos. Mater.* **2012**, *2*, 17–21.

(31) Lehr, B.; Bristol, S.; Possolo, A. *Oil Budget Calculator: Deepwater Horizon*; available via the Internet at http://noaa.ntis.gov/view.php?pid=NOAA:ocn690106535 (accessed Nov. 25, 2014).

(32) Aveyard, R.; Binks, B. P.; Clint, J. H. Emulsions Stabilised Solely by Colloidal Particles. *Adv. Colloid Interface Sci.* **2003**, *100–102*, 503–546.

(33) Melle, S.; Lask, M.; Fuller, G. G. Pickering Emulsions with Controllable Stability. *Langmuir* **2005**, *21*, 2158–2162.

DOI: 10.1021/acs.chemmater.5b01523
Chem. Mater. 2015, 27, 3775–3782

(34) Zhou, J.; Qiao, X.; Binks, B. P.; Sun, K.; Bai, M.; Li, Y.; Liu, Y. Magnetic Pickering Emulsions Stabilized by Fe_3O_4 Nanoparticles. *Langmuir* **2011**, *27*, 3308−3316.
(35) Kaiser, A.; Liu, T.; Richtering, W.; Schmidt, A. M. Magnetic Capsules and Pickering Emulsions Stabilized by Core−Shell Particles. *Langmuir* **2009**, *25*, 7335−7341.
(36) Brown, P.; Butts, C. P.; Cheng, J.; Eastoe, J.; Russell, C. A.; Smith, G. N. Magnetic Emulsions with Responsive Surfactants. *Soft Matter* **2012**, *8*, 7545−7546.

DOI: 10.1021/acs.chemmater.5b01523
Chem. Mater. 2015, 27, 3775−3782